

Quantitative shear wave imaging of cell culture gels

Marko Orescanin,^{1,3} Kathleen S. Toohey,^{2,3} and Michael F. Insana^{1,2,3}

¹Department of Electrical and Computer Engineering, ²Department of Bioengineering

³Beckman Institute for Advanced Science and Technology

University of Illinois at Urbana-Champaign, Urbana, Illinois 61801

Email: moresca2@illinois.edu

Abstract—An ultrasonic shear wave imaging technique is being developed for estimating viscoelastic properties of hydrogels. A needle placed in the medium is vibrated along its axis to generate harmonic shear waves. Doppler pulses synchronously track shear wave propagation to estimate the local speed. Fitting shear-wave speed estimates to the dispersion relation obtained from two rheological models, we estimate the complex shear modulus, viz., elastic and viscous components. The dispersion equation estimated using the standard solid-body (Zener) model is compared to that from the Kelvin-Voigt model to explore the frequency landscape of hydrogel viscoelasticity within the 50-450 Hz shear wave bandwidth. We found both models give comparable estimates that each agree with independent rheometer measurements obtained at lower strain rates, as might be expected from these highly elastic gels.

I. INTRODUCTION

Elasticity imaging techniques have shown great potential for assessing the mechanical environment surrounding malignant mammary cells, and yet the mechanisms responsible for in vivo elasticity breast imaging contrast remain poorly understood. Epigenetic factors, such as the mechanical properties of extracellular matrix (ECM) – interstitial fluid interactions, and the presence of signaling proteins, work together to determine the growth rate of transformed cells that initiate malignant breast tumors [1]. Because genetically transformed cells are encouraged to grow and form malignant tumors when placed in a stiff mechanical environment, images of viscoelastic properties convey important diagnostic information. The biphasic nature of the mechanical response, whereby solid ECM polymers are surrounded by interstitial fluids, suggest that breast tissues may respond as a poro-viscoelastic material. The degree of poroelasticity versus viscoelasticity depends strongly on the strain rate, as determined by the shear wave frequency. Interactions between fluids flowing through the polymer, and their spatial variations, is the most likely cause for contrast in the elasticity images. Consequently, we are exploring contrast mechanisms by developing techniques that extend our quasi-static (< 1 Hz) measurements to higher shear-wave frequencies.

The initial study summarized in this report is to develop the measurement technique. It focuses on elastic collagen hydrogels of the type using for 3-D cell cultures. They have a weak viscoelastic responses, mostly elastic, but they are well studied materials. The basic measurement is also well-known: a Doppler probe tracks shear wave particle motion that leads to the estimation of local shear-wave speed. Assuming a

rheological model, dispersion equations are derived that are fit to the speed measurements to estimate the complex modulus, $\mu = \mu_1 - i\omega\eta$, where μ_1 is the elasticity shear modulus and η is the viscous shear modulus. Here, the accuracy of the estimation techniques are tested for a largely elastic response. In a second report at this conference, however, we apply these methods to liver tissues where we find a strong viscoelastic response and model dependent differences.

II. METHODS

A. Experimental setup

The shear wave imaging experiment is diagrammed in Fig. 1. A mechanical actuator harmonically vibrates a 1.5-mm-dia needle along the z axis at single frequencies in the range of 50-450 Hz. Narrow-band shear waves radiate cylindrically from the needle and are imaged in the x, z plane using a linear-array, pulsed-Doppler probe (SonixRP, BW-14/60, Ultrasonix Medical Corporation, Richmond, BC). The axes of the needle and linear-array beam are separated by angle θ . This type of excitation is efficient at generating shear waves in the medium, giving a high echo SNR for Doppler estimates over a region of several square millimeters.

B. Doppler estimation

The Doppler probe was excited by 6-cycle pulses at a center frequency $f'_c = 6.67$ MHz. The nominal echo frequency was $f_c = 6$ MHz, which is used for velocity calculations in the following analysis. Shear wave excitation and Doppler acquisitions were synchronized. In the lower half of the Fig. 1 we present a Doppler acquisition timing diagram. A packet of 3000 pulse-echo acquisitions was obtained at a pulse repetition frequency PRF = 10 kHz for a total acquisition time at each line of sight of $T_s = 300$ ms. Subsequently, the beam-axis was translated along the array by an element pitch and the acquisition was repeated until we obtained the entire field of view for each shear wave frequency.

Particle velocity is estimated from the phase shift measured between Doppler echoes during shear wave propagation. The standard Kasai velocity estimator is based on lag-one echo correlation using pulse-pair processing [2]. Our harmonic shear waves generate a narrow-band Doppler spectrum at low Doppler frequencies (< 500 Hz), which increases the inter-pulse correlation for the ensemble and thus provides an opportunity to extend the lag-one correlation approach for

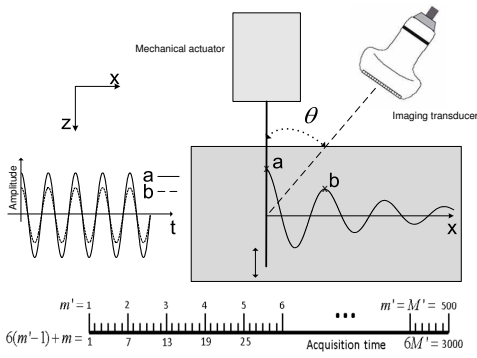


Fig. 1. The shear wave imaging experiment is depicted. A mechanical actuator harmonically drives a stainless steel needle which is the source of cylindrical shear waves. A linear array tracks the shear wave via pulsed Doppler methods. In the lower half of the figure, Doppler acquisition scheme is illustrated.

reducing estimation variance. Specifically, we adopted the lag- k estimator that averages estimates of the linear phase at k time lags [3]. The variance of velocity estimates is lowered because the echo noise is zero mean and signal independent.

We collected $M' = 500$ ensembles of $M = 6$ pulses where $1 \leq m' \leq M'$. Each ensemble provides a single phase estimate. We compute the complex echo waveform $V[\ell, n, m]$ from the RF data, where index $1 \leq \ell \leq L$ counts A-lines along the lateral direction, index $1 \leq n \leq N$ counts samples along the axial direction (fast time), and index $1 \leq m \leq M$ counts echo waveforms in the ensemble (slow time).

We estimate the k -lag correlation function between elements of the ensemble via

$$\hat{\phi}_k[\ell, n, m'] = \frac{1}{M-k} \sum_{m=1}^{M-k} V_{m'}^*[\ell, n, m] V_{m'+k}[\ell, n, m+k], \quad (1)$$

where $1 \leq k \leq P < M$. To estimate the echo phase, we combine individual k -lag estimates in a manner that resolves the phase ambiguity,

$$\arg(\hat{\phi}[\ell, n, m']) = \frac{1}{P} \sum_{k=1}^P \frac{1}{k} \arg(\hat{\phi}_k[\ell, n, m']). \quad (2)$$

The instantaneous velocity \hat{v} is therefore [2], [4]

$$\hat{v}[\ell, n, m'] = \left(\frac{-c}{4\pi f_c T_{prf} \cos \theta} \right) \arg(\hat{\phi}[\ell, n, m']) \quad (3)$$

where c is the compressional-wave speed of sound in the gel medium (1.5 mm/ μ s) and $\arg(\cdot)$ indicates the phase angle obtained from the arctangent of the ratio of imaginary to real parts of the argument.

Selecting $P = 1$, Eq. (2) and (3) are reduced to the standard lag-one autocorrelation estimator [2], [4]. In the work presented below, we set $P = 5 = M - 1$.

C. Phase gradient estimator

There is a simple analytic solution to the wave equation that describes harmonic cylindrical shear waves propagating

from a long needle in a homogeneous medium [5]. It gives the particle displacement along the x -axis (see Fig 1) as

$$u(x, t) = \frac{i}{4} H_0^{(1)}(k_s x) e^{-i\omega t}. \quad (4)$$

where $H_0^{(1)}$ is the zeroth-order Hankel function of the first kind, x is the radial distance from the needle in the x, y plane, k_s is the shear wave number at radial frequency ω . Particle velocity is found from the time derivative of Eq. (4),

$$v(x, t) = \frac{w}{4} H_0^{(1)}(k_s x) e^{-i\omega t}. \quad (5)$$

For large $k_s x$, $H_0^{(1)} \rightarrow \sqrt{\frac{2}{\pi k_s x}} e^{i(k_s x - \pi/4)}$ [6]. Thus, after much algebra, it can be shown that Eq. (5) is approximately

$$v(x, t) = \frac{w}{4} \sqrt{\frac{2}{\pi k_s x}} e^{i(k_s x - \omega t - \frac{\pi}{4})} = V_0(x) e^{i\beta(t)} e^{i\zeta(x)}. \quad (6)$$

$V_0(x)$ is the spatially-varying velocity magnitude; it is multiplied by temporal and spatial phase terms. The spatial phase factor for particle velocity is a linear function of x . Its first derivative is

$$\frac{d\zeta}{dx} = \frac{\omega}{c_s}. \quad (7)$$

Thus shear wave speed is estimated from the spatial phase gradient of particle velocity as measured from Doppler signals. In practice, the x axis is sampled according to the array pitch $\Delta x = 460 \mu\text{m}$, such that $x = \ell \Delta x$.

Beginning with the expression for particle velocity from Eq (3), we compute its analytic signal, $\hat{v}'[\ell, n, m']$, so that we can estimate the spatial phase between lateral echo lines, via index ℓ , in the direction of the linear array elements. Defining a spatial ensemble of $L = 4$ lateral echo lines, we compute the lag-one correlation estimate for the ensemble using

$$\hat{\psi}[\ell', n, m'] = \frac{1}{L-1} \sum_{\ell=1}^{L-1} \hat{v}'_{\ell'}^*[\ell, n, m'] \hat{v}'_{\ell'}[\ell+1, n, m']. \quad (8)$$

We then drop the left-most echo line and add the next adjacent echo line to the right and repeat estimates over index ℓ' . For 128 lateral echo lines in an acquisition frame, we can obtain as many as 121 spatial phase estimates using this running average technique.

Jensen [2] showed, after considerable algebra, that $d\zeta/dx$ from (7) is approximately $(\arg \hat{\psi})/\Delta x$ from (8). Thus (7) gives

$$\hat{c}_s[\ell', n, m'] = \frac{\omega \Delta x}{\arg(\hat{\psi}[\ell', n, m'])} \quad (9)$$

Choose a region of interest (ROI) close to the needle, the mean and standard deviation for c_s is estimated at each ω . Shear wave dispersion relations connect c_s to the complex modulus, as we now show.

D. Shear wave dispersion

Harmonic shear wave propagation in complex media is governed by frequency of excitation and material properties. An important quantity for the shear wave motion analysis is a complex shear wave number $k_s = (\rho\omega^2/\mu)^{1/2}$, where ρ is the mass density, ω is the angular shear-wave frequency, and μ is the complex shear modulus of the material. The complex wave number can be written as a function of the shear wave speed and shear wave attenuation constant $k_s = \omega/c_s - i\alpha_s$. Material properties are related to c_s through rheological models of mechanical behavior.

The Kelvin-Voigt model, Fig. 2, is commonly used to describe viscoelastic effects for shear wave imaging application. Complex modulus of the Kelvin-Voigt model is $\mu^K(\omega) = \mu_1 - i\omega\eta_K$ where μ_1 is the relaxed modulus ($\mu^K|_{\omega \rightarrow 0} = \mu_1$) and η_K is the viscous component. We compared Kelvin-Voigt model with a standard solid model or Zener model, Fig. 2, which is often used to represent polymer dynamics [7]. The complex modulus of the Zener model is given by

$$\mu^Z(\omega) = \mu_1 \frac{1 + \omega^2\tau_\sigma\tau_\epsilon}{1 + \omega^2\tau_\sigma^2} - i\omega\mu_1 \frac{\tau_\epsilon - \tau_\sigma}{1 + \omega^2\tau_\sigma^2}, \quad (10)$$

where $\mu_1 = \mu^Z|_{\omega \rightarrow 0} = k_1k_2/(k_1+k_2)$ is the relaxed modulus and $\tau_\sigma = \eta_Z/(k_1+k_2)$ and $\tau_\epsilon = \eta_Z/k_2 \geq \tau_\sigma$ are the relaxation times, respectively.

Shear wave speed and attenuation can be calculated with the same analytical expressions for both models

$$\begin{aligned} c_s^{K,Z}(\omega) &= \omega/\Re\{k_s^{K,Z}\} \\ &= \sqrt{\frac{2(\Re\{\mu^{K,Z}\}^2 + \Im\{\mu^{K,Z}\}^2)}{\rho(\Re\{\mu^{K,Z}\} + \sqrt{\Re\{\mu^{K,Z}\}^2 + \Im\{\mu^{K,Z}\}^2})}} \end{aligned} \quad (11)$$

and

$$\begin{aligned} \alpha_s^{K,Z}(\omega) &= \Im\{k_s^{K,Z}\} \\ &= \sqrt{\frac{\rho\omega^2(\sqrt{\Re\{\mu^{K,Z}\}^2 + \Im\{\mu^{K,Z}\}^2} - \Re\{\mu^{K,Z}\})}{2(\Re\{\mu^{K,Z}\}^2 + \Im\{\mu^{K,Z}\}^2)}} \end{aligned}, \quad (12)$$

where indexes K or Z denote Kelvin-Voigt or Zener model respectively. [8], [9]

Frequency characteristic of viscous losses are often quantified by the quality factor $Q(\omega) = -\Re\{k_s^2\}/\Im\{k_s^2\}$ whose inverse Q^{-1} , is called the dissipation factor. For Kelvin-Voigt model $Q^K(\omega) = 1/(\omega\tau)$ where $\tau = \eta_Z/\mu_1$ and for Zener model $Q^Z(\omega) = (1 + \omega^2\tau_\epsilon\tau_\sigma)/\omega(\tau_\epsilon - \tau_\sigma)$.

III. RESULTS

Experiments were conducted on homogenous hydrogel phantoms of 4% and 8% gelatin concentrations. Three samples were tested for 4% concentration and two samples for 8% concentration. Speed measurements were averaged separately for both concentrations. We conducted rheometer experiments to independently estimate the storage modulus at both gel concentrations. Five samples were measured at each concentration and averaged.

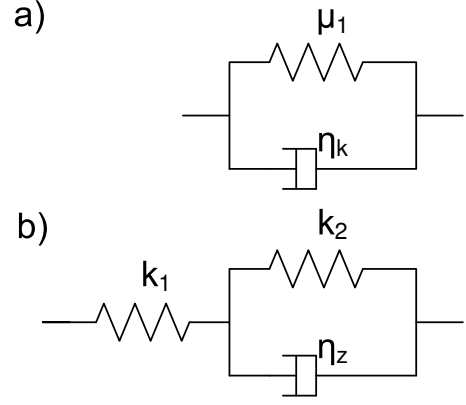


Fig. 2. (a) The Kelvin-Voigt model is diagrammed. Model consists of an elastic component μ_1 in parallel with the viscous component η_k . (b) The standard linear solid or Zener model is illustrated. It is a series combination of elastic and Kelvin-Voigt units.

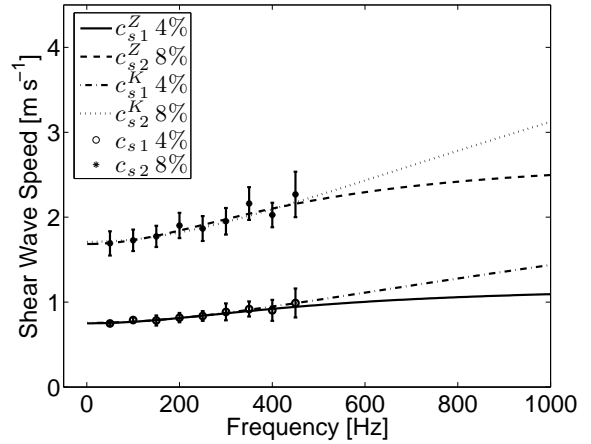


Fig. 3. Comparison of shear wave speeds as a function of frequency for the Kelvin-Voigt model and the Zener model at two gelatin concentrations, 4% and 8%. Models are consistent at low frequencies but diverge above 500 Hz.

In Fig.(3), we present c_s measurements for both gel concentrations. These data are numerically fit to Eq. (11) via nonlinear regression for the Kelvin-Voigt and Zener models. The shear speed for both models approaches the low frequency limit of $c_s^{K,Z}(0) = \sqrt{\mu_1/\rho}$, monotonically increasing with ω . The Kelvin-Voigt model give a speed that is unbounded, $c_s^K(\omega)|_{\omega \rightarrow \infty} = \infty$, whereas the Zener model is bounded by the unrelaxed modulus, $c_s^Z(\omega)|_{\omega \rightarrow \infty} = \mu_U = \mu_1(\tau_\epsilon/\tau_\sigma)$. The two models overlap within measurement error over the measurement bandwidth.

Fit parameters are listed in Table I. At the 4% gelatin concentration, we find agreement within 3% among relaxed moduli estimated using the two rheological models to that from the rheometer. At 8% gelatin concentration, the agreement is within 22%, which is consistent with our previous findings that inter-sample variability dominates at 20% of the mean. The variabilities are primarily because of gel preparation [10].

In Fig.(4), the predicted dissipation factor is evaluated between 0 and 10^4 Hz for the average moduli estimated for both

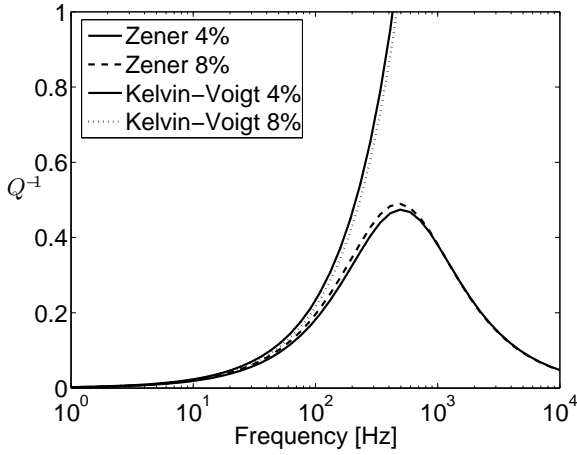


Fig. 4. Dissipation factor as a function of frequency for the Kelvin-Voigt model and the Zener model for two gelatin concentrations of 4% and 8%.

TABLE I
ESTIMATED VISCOELASTIC PARAMETERS

Model	μ_1 [Pa]	η_K [Pa s]	k_1 [Pa]	k_2 [Pa]	η_Z [Pa s]
<i>Gel.</i> 4%					
<i>KV</i>	570	0.21			
<i>Zen.</i>	563		1407	938	0.47
<i>Rh.</i>	571 ± 67				
<i>Gel.</i> 8%					
<i>KV</i>	2919	1.0			
<i>Zen.</i>	2836		7288	4642	2.46
<i>Rh.</i>	2286 ± 315				

models and at both gelatin concentrations. Both gels are highly elastic at low frequency, and there is little difference between models below 500 Hz. At higher frequencies, the Kelvin-Voigt model predicts increasing dissipation whereas the Zener model predicts decreasing dissipation, ultimately becoming elastic behavior at frequencies greater than 1 kHz. The relaxation peak of the Zener model is located at $f_0 = 1/(2\pi\tau_0)$ where $\tau_0 = \sqrt{\tau_\epsilon\tau_\sigma}$ and represents a peak of viscous losses. For the estimated properties for 4% and 8% gelatin estimated relaxation peaks are located at $f_0^{4\%} = 503$ Hz and $f_0^{8\%} = 481$ Hz, respectively.

IV. CONCLUSION

A shear wave imaging method based on the Doppler estimation of shear wave propagation excited by the vibrating needle is presented. Quantitative estimation of the viscoelastic properties is demonstrated on soft gelatin samples. We show how to relate parameters of the Kelvin-Voigt model used to quantify material response to the shear wave propagation to parameters obtained with rheometer tests. Moreover, we have considered the higher-order Zener model for characterizing hydrogel response within the given bandwidth of the measurement.

Within the testing bandwidth, hydrogel exhibits strong elastic behavior and differences between the two models is

negligible. Therefore either model is representative of gelatin gels between 4% and 8% concentrations. Increasing the measurement bandwidth above 450 Hz would provide a means to differentiate between the two models. Soft biological tissues have a greater viscoelastic response than gels and therefore it may be clear which of the two rheological models best represents the mechanical responses in the 50-450 Hz range.

ACKNOWLEDGMENT

The authors gratefully acknowledge Rousselot Inc., Dubuque, IA, for providing a generous supply of gelatin in support of this research, the Autonomic Materials Laboratory at the Beckman Institute for use of a rheometer, and the Bioacoustics Research Laboratory at the Beckman Institute for allowing use of their facilities. We gratefully acknowledge the support of Dr. Lianjie Huang and the U.S. Department of Energy through the LANL/LDRD Program for this work. This work was supported by the National Cancer Institute under award number R01 CA082497.

REFERENCES

- [1] R.A. Weinberg, *The Biology of Cancer*, Garland, New York, 2006.
- [2] J. A. Jensen, *Estimation Of Blood Velocities Using Ultrasound: A Signal Processing Approach*, Cambridge University Press, New York, 1996.
- [3] P.R. Mahapatra and D.S. Zrnic, "Practical algorithms for mean velocity estimation in pulse Doppler weather radars using a small number of samples," *IEEE Transactions on Geoscience and Remote Sensing*, vol. GE-21, pp. 491-501, October 1983.
- [4] R.J. Doviak and D.S. Zrnic, *Doppler Radar And Weather Observations, 3/e*, Academic Press Inc., San Diego, 1993.
- [5] K.F. Graff *Wave Motion In Elastic Solids*, Dover Publications, Inc., New York, 1991.
- [6] L.E. Kinsler, A.R. Frey, A.B. Coppens, J.V. Sanders, *Fundamentals of Acoustic 4/e*, Wiley, New York, 2000.
- [7] J.M. Carcione *Wave Fields in Real Media: Wave Propagation in Anisotropic, Anelastic and Porous Media*, Elsevier Science Ltd., Oxford, 2001.
- [8] E.L. Madsen, H.J. Sathoff, J.A. Zagzebski, "Ultrasonic shear wave properties of soft tissues and tissuelike materials," *J Acoust Soc Am*, 74:1346-1355, 1983.
- [9] S. Chen, Member, M. W. Urban, C. Pislaru, R. Kinnick, Y. Zheng, A. Yao, and J. F. Greenleaf, "Shearwave Dispersion Ultrasound Vibrometry (SDUV) for Measuring Tissue Elasticity and Viscosity," *IEEE Trans. Ultrason. Ferroelectr. Freq. Control*, vol. 56, no. 1, pp. 55-62, 2009.
- [10] M. Orescanin, K. S. Toohy, and M. F. Insana, "Material properties from acoustic radiation force step response," *J. Acoust. Soc. Am.*, vol. 125, no. 5, pp. 2928-2936, 2009.
- [11] P.T. May, T. Sato, M. Yamamoto, S. Kato, T. Tsuda and S. Fukao, "Errors in the determination of wind speed by Doppler Radar," *Journal of Atmospheric and Oceanic Technology*, vol. 6, pp. 235-242, April 1984.
- [12] K. Hoyt, K. J. Parker and D. J. Rubens, "Real-time shear velocity imaging using sonoelastographic techniques," *Ultrasound in Med. & Biol.*, Vol. 33, No. 7, pp. 1086-1097, 2007.
- [13] S. Chen, M. Fatemi and J. F. Greenleaf, "Quantifying elasticity and viscosity from measurement of shear wave speed dispersion," *J. Acoust. Soc. Am.*, Vol. 115, No. 6, pp. 2781-2785, 2004.